

# STUDY OF THE EFFECT OF $B_2O_3$ - $Bi_2O_3$ GLASS ADDITIVE ON STRUCTURAL AND DIELECTRIC BEHAVIOUR OF $Ba_{0.5}Sr_{0.5}TiO_3$ CERAMIC

---

## 6.1 Introduction

The perovskite ceramics have attracted greater attention in recent years due to demand for microwave devices, dielectric resonators (DRS), solid fuel cells and other components [Sebastian (2008); (Lekshmi et al. (2018); Coronado et al. (2014)]. Barium strontium titanate (BST) ceramic is one of the promising perovskite ceramics that gives high dielectric constant and low dielectric loss. It shows good tunability, tunable transition temperature, and better mechanical and thermal responses. It is used in a wide range of applications such as in devices/ components including sensors, dielectric resonators, tunable filters, transducers, phase shifters, capacitors, thermistors, oscillators, dielectric layers in electroluminescent displays [Brankovic et al. (2005)] due to exhibition of temperature dependent ferroelectric and paraelectric natures.  $BaTiO_3$  shows ferroelectric phase at room temperature but changes to paraelectric phase above the transition temperature. Moreover,  $SrTiO_3$  has transition temperature near the absolute zero. But in solid solution of BST, with varying the ratio of Ba to Sr, Curie temperature show linear variation with increasing fraction of Strontium. Paraelectric phase of BST can be preferably used to avoid ageing and fatigue because of ferroelectric domain switching for microwave devices.  $Ba_{1-x}Sr_xTiO_3$  (where  $x=0.4$ ) material shows transition temperature below room temperature [Jeon (2004); Alexandru et al. (2006); Yu et al. (2013)] and so it exhibits paraelectric phase at room temperature. BST has Curie temperature below room temperature. It undergoes three different phase transitions similar to  $BaTiO_3$  (cubic-

tetragonal-orthorhombic-rhombohedral) but the transitions are shifted to lower temperatures. Only cubic structure is paraelectric and all other structure are ferroelectric [Jona and Shirane (1993)].

Perovskite ceramics with low sintering temperature are in more demand for the manufacturing of next generation low cost ceramic products, such as substrates, multichip modules and microwave components/devices [Tagantsev et al. (2003); Sherman et al. (2006); Maiti et al. (2006); Varghese et al. (2018); Joseph et al. (2018)]. Several methods including chemical synthesis, high energy ball milling and liquid phase sintering are used for lowering the sintering temperature to reduce the manufacturing cost. In liquid phase sintering, addition of low melting point glass to ceramic is one of the best methods for decreasing the sintering temperature without degrading the ceramic properties [Varghese et al. (2016)]. The liquid phase of glass makes a bridge between grain and penetrates the solid particles to shear uniformly. The driving force enhances the compaction resulting in increase of its density. However, glass also possesses some inherent properties, such as high durability, low melting temperature, low viscosity and non-reactivity with ceramic materials. Moreover, in  $\text{Bi}_2\text{O}_3\text{-B}_2\text{O}_3$  glasses,  $\text{B}_2\text{O}_3$  is one of important glass formers which is incorporated into various kinds of glass system as flux. The boron atom usually coordinates with either three or four oxygen atoms in borate crystal and glass, forming  $(\text{BO}_3)$  or  $(\text{BO}_4)$  structural units. The number of structure units depends on total concentration of added modification and its nature [Shelby (1997); Varshneya (1994); Yano et al. (2003); Stone et al. (2000); Stehle et al. (1998)] and other term  $\text{Bi}_2\text{O}_3$  is a higher valency oxide and has low field strength and high polarization, due to this reason glassy phase cannot be obtained in contrast to pure  $\text{B}_2\text{O}_3$  glass. Moreover, it may build a glass network of  $(\text{Bi}_2\text{O}_3)$  pyramids in presence of small amount addition of conventional glass formers e.g.  $(\text{Bi}_2\text{O}_3)$ . Therefore,  $\text{Bi}_2\text{O}_3\text{-B}_2\text{O}_3$  glass provides a large glass forming

range with stable thermal and physical properties [Baia et al. (2003); Simon and Todea (2006); Gowda et al. (2007)].

In the present investigation, novel  $45\text{Bi}_2\text{O}_3\text{-}55\text{B}_2\text{O}_3$  (BB) glass is synthesized and utilized as the sintering aid for  $\text{Ba}_{0.5}\text{Sr}_{0.5}\text{TiO}_3$  (BST) ceramic. The effects of BB glass addition on the sintering temperature, phase and dielectric properties of BST ceramic are investigated comprehensively.

## 6.2 Results and Discussion

The synthesis of  $45\text{Bi}_2\text{O}_3\text{-}55\text{B}_2\text{O}_3$  (BB) glass added  $\text{Ba}_{0.5}\text{Sr}_{0.5}\text{TiO}_2$  (BST) ceramic was performed by solid state method. The detailed synthesis process has been mentioned in section 3.1(Sub-section 3.1.1, 3.1.2, 3.1.3, and 3.1.4(b)) of chapter 3. The nomenclature of different BST-BB batch compositions is given in Table 6.1. The detailed specification and description of the equipments used for material characterisation, such as density, phase, microstructure and dielectric properties are mentioned in section 3.2 of chapter 3.

**Table 6.1** Nomenclature of different BST-BB batch compositions

S.No.	Sample Composition	Nomenclature
1.	BST with 0 wt% glass	BST
2.	BST with 3 wt% glass	BST-3B
3.	BST with 5 wt% glass	BST-5B
4.	BST with 8 wt% glass	BST-8B
5.	BST with 10 wt% glass	BST-10B

### 6.2.1 Thermo-gravimetric and differential thermal analysis

The detailed analysis of TG/DTA plot of ball milled powder of  $\text{Ba}_{0.5}\text{Sr}_{0.5}\text{TiO}_3$  (BST) batch was done in section 4.31 of chapter 4. Figure 6.1 shows the DTA thermogram for  $45\text{Bi}_2\text{O}_3\text{-}55\text{B}_2\text{O}_3$  (BB) glass recorded in temperature range 423-1073 K. The first endothermic peak is observed at around 715 K, depicting the glass transition temperature

( $T_g$ ). Two distinct and broad exothermic peaks at around 754 K and 804 K are observed representing the first  $T_{c1}$  ( $Bi_2O_3$  phase) and second  $T_{c2}$  ( $B_2O_3$  phase) crystallization respectively. Furthermore, two endothermic peaks were observed at around 880 K (for  $Bi_2O_3$ ) and 1012 K ( $B_2O_3$ ) corresponding to melting temperature of first ( $T_{m1}$ ) and second ( $T_{m2}$ ) crystallization respectively.  $Bi_2O_3$ - $B_2O_3$  glasses provide large glass forming range with stable thermal and physical properties [Lee et al., (2005)].  $Bi_2O_3$  has attracted considerable attention because it occupies both network forming and network modifying positions in the borate glass and the addition of small concentration of network modifier to the  $B_2O_3$  increases the glass transition temperature [Avramov et al. (2005)].

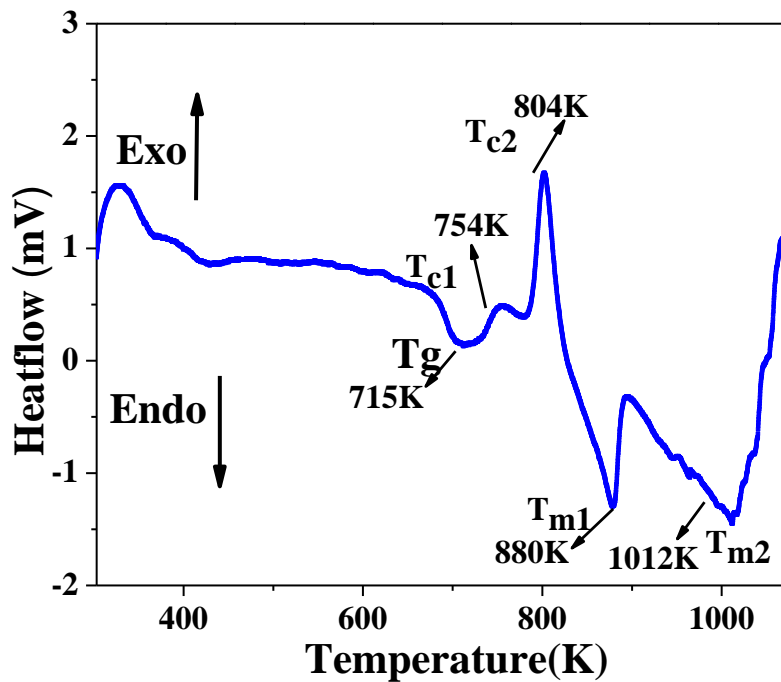


**Figure 6.1** DTA/TGA of BB glass.

## 6.2.2 Sintering and densification behaviour

Figure 6.2 shows the variations of percent relative density as a function of sintering temperature for all glass added BST (BST-3B, BST-5B, BST-8B and BST-10B) compositions. The inset of figure 6.2 shows the variation of density with sintering temperature for the BST ceramics. The pure BST ceramic specimen was sintered in the temperature range 1300-1600 K and different glass added BST ceramic specimens were sintered in the temperature range 1148 - 1273K. Maximum percentage density of 96.42% is obtained for the BST-5B ceramic, which was sintered at 1223 K. The density of BB glass and BST were obtained as  $6.13 \text{ g/cm}^3$  and  $5.627 \text{ g/cm}^3$  respectively. It was found that the density of all the compositions increases with increasing sintering temperature up to a particular temperature and thereafter it decreases. Decrease in density after reaching certain maximum value may be due to the excessive grain growth and crystallization of glass, reducing densification and increasing porosity [Anjana and Sebastian (2009)]. The maximum relative percentage densities for different compositions at their optimum sintering temperatures are given in Table 6.2. The value of density increases with increasing concentration of glass upto 5% and after that it decreases. The increasing concentration of glass above 5% leads to transient liquid phase and swelling of compact causes decrease in density. It is observed from the graph that the addition of glass phase accelerates the densification of BST ceramic at significant lower sintering temperatures. Low sintering temperature of the ceramic is preferred as it reduces the production cost at medium to large scale. Addition of glass increases the density because liquid form of glass penetrates the solid particles of ceramic to spread uniformly, fill the pores and form bridges between the grains.

**Table 6.2** The maximum relative percentage densities for different compositions

Sample Code	Sintering Temperature	Relative Density (%)
BST	1523 K	92.06
BST-3B	1223 K	92.43
BST-5B	1223 K	96.42
BST-8B	1223 K	95.08
BST-10B	1223 K	93.65

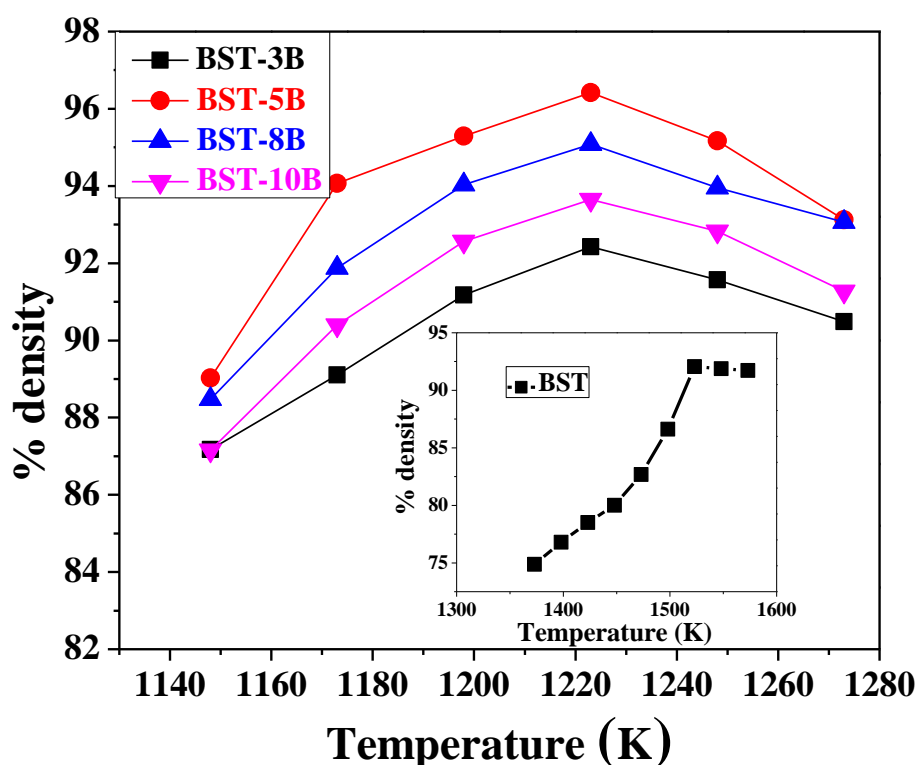


**Figure 6.2** Variations of density of BST, BST-3B, BST-5B, BST-8B and BST-10B samples with sintering temperature.

### 6.2.3 Phase analysis

The X-ray diffraction (XRD) patterns of the calcined and sintered ceramic samples (BST, BST-3B, BST-5B, BST-8B and BST-10B) were recorded via X-ray Diffractometer (Rigaku MiniflexII, Desktop X-Ray D) using Cu K $\alpha$  ( $\lambda = 1.541836 \text{ \AA}$ ) radiation with Ni filter. All the XRD peaks of BST ceramic were matched with the JCPDS file no. 39-1395. Rietveld refinement was also performed using FullProf\_Suite. The phase analysis of XRD peaks of BST ceramics has been explained in detail in section 4.2.3 of chapter 4.

Figure 6.3 shows the comparative XRD patterns of liquid phase sintered BST samples (BST-3B, BST-5B, BST-8B and BST-10B). No secondary peak is observed in the XRD patterns. It is clear from figure 6.3 that addition of different wt% (3, 5, 8, and 10) of glass has no effect on the diffraction pattern and crystal structure of BST phase.

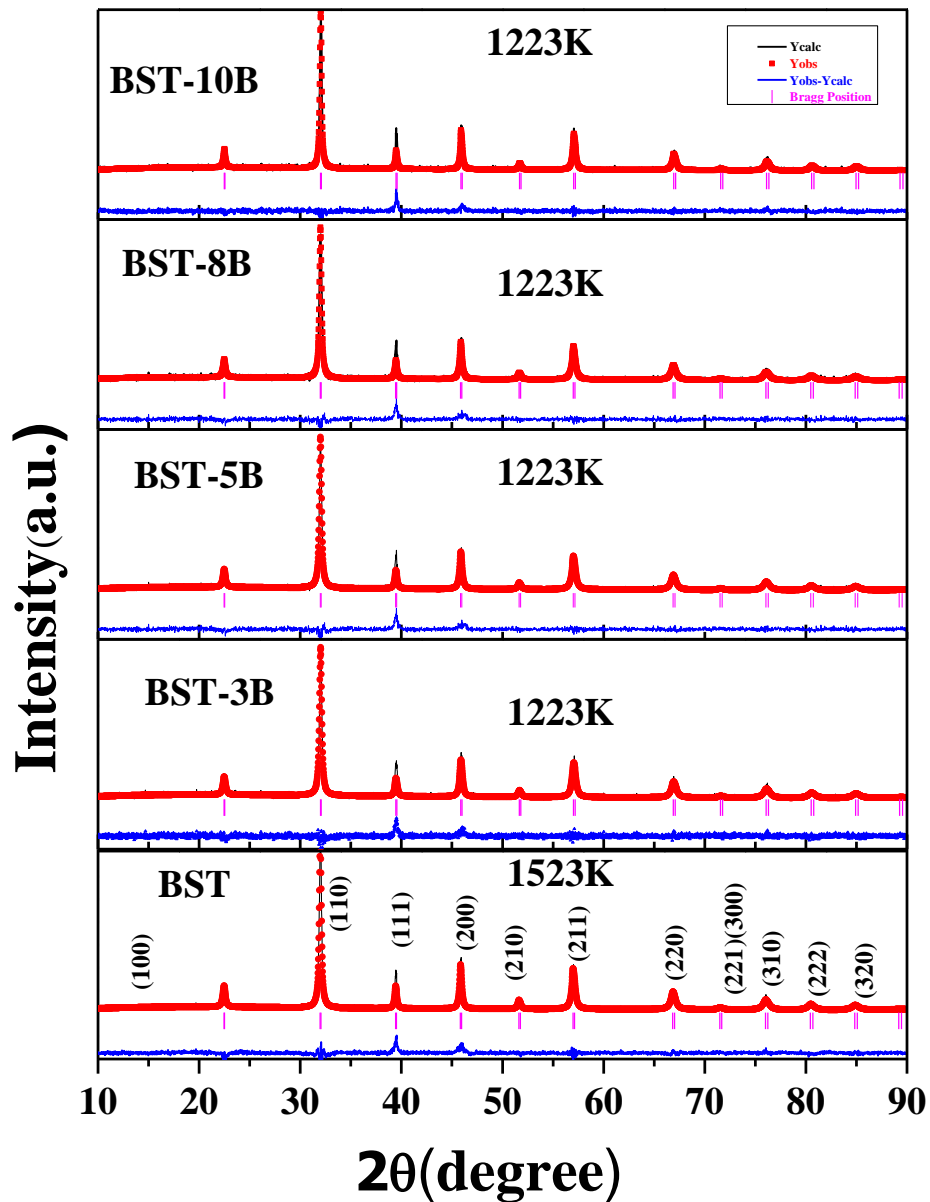


**Figure 4.3(c)** Comparative XRD analysis of BST, BST-3P, BST-5P, BST-8P and BST-10P samples sintered at 1523K, 1223K, 1198K, 1173K and 1148K respectively.

#### 6.2.4 Microstructure

Figure 6.4 shows SEM microstructures of all liquid phase sintered BST samples (BST-3B, BST-5B, BST-8B and BST-10B) at 30K magnification. The microstructures clearly show the grain growth in all samples with average grain size in micrometre range. Exaggerated grain growth ( $\sim 0.8 \mu\text{m}$ ) and heterogeneous grain distribution in BST ceramic sample is clearly shown in figure 6.4 (a). BST-3B and BST-5B ceramics have average grain size of  $\sim 0.38 \mu\text{m}$  and  $\sim 0.39 \mu\text{m}$  respectively along with homogeneous distribution throughout the ceramic mixture as shown in figure 6.4(b and c). Figure 6.4 (d) of (BST-8B) ceramic shows that grain size reduces remarkably, which may be due to diffusion of glass in pores. However, the microstructure of BST-10B shows that samples become more porous due the re-crystallization process with average grain size of about  $0.42 \mu\text{m}$ . From figure 6.4 (b-e), it is observed that liquid phase sintering reduces the average grain size of the sample due to decrease of sintering temperature when compared with solid-state sintering (as shown in Figure 6.4 (a)). For glass addition with BST sample, the results shown in figure 6.4(b-e), indicate that the grain uniformly decreases with increase in weight percent of glass, which can be attributed to liquid phase effect of glass observed at grain boundaries. Sample (BST-5B) shows maximum density, which is also verified from measured and theoretical densities. It may be concluded that the glass concentration plays an important role in densification and homogenization and reduces the grain size of BST. Therefore, glass is regarded to act as an effective sintering aid for BST ceramics.

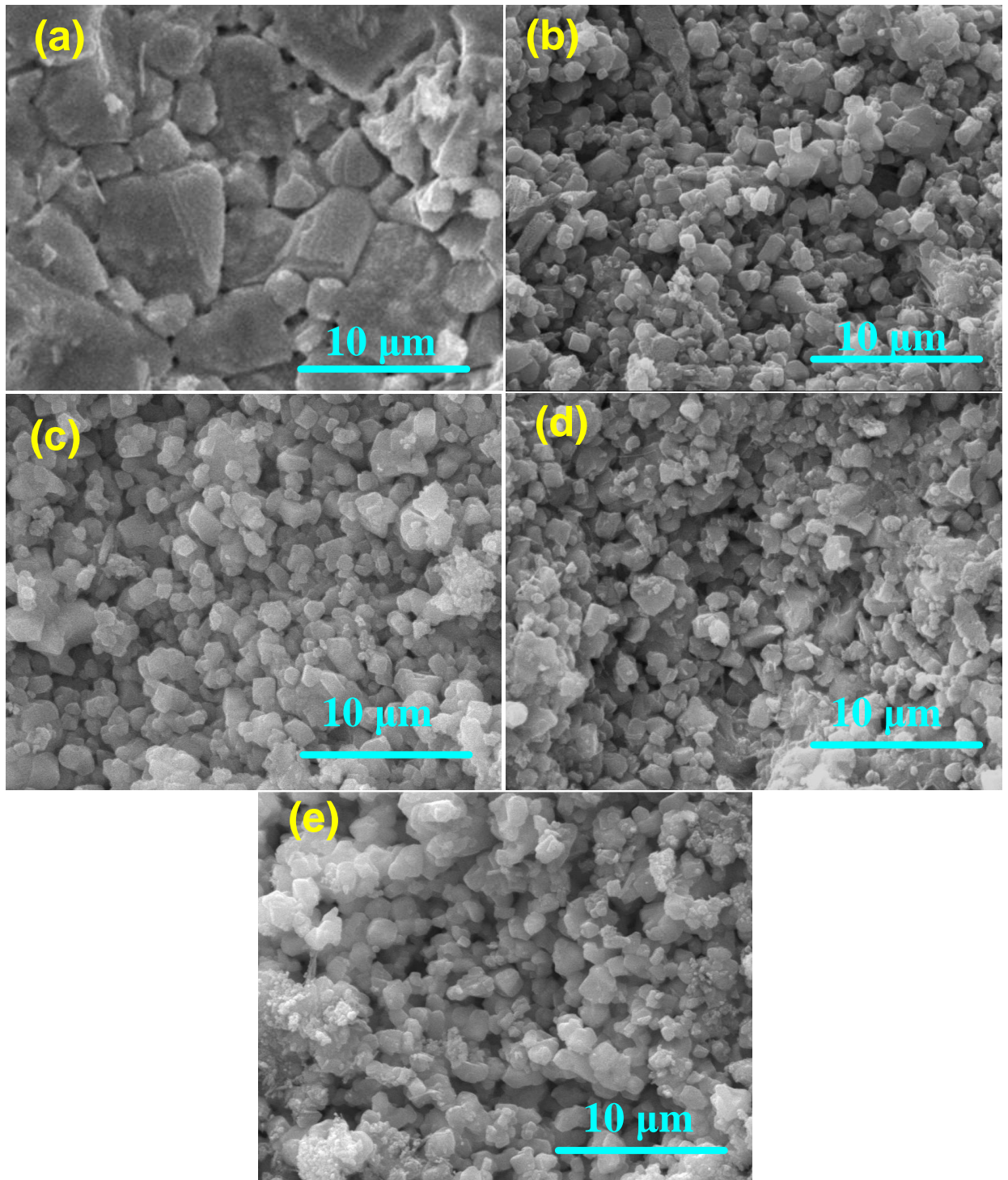


**Figure 6.4** SEM microstructure of (a) BST, (b) BST-3B, (c) BST-5B, (d) BST-8B and (e) BST-10B.

### 6.2.5 Analysis of dielectric property

The measured temperature dependent dielectric constant and loss tangent (inset) at different frequencies (1 KHz, 10 KHz, 100 KHz, 500 KHz and 1 MHz) are shown in figures 6.5 and 6.6 for all sintered samples (BST-BST-10B) within the temperature range 20K-290K and 293K-500K respectively. It is observed from figure 6.5(a-e) that dielectric constant value increases with increasing temperature up to the transition temperature. This trend is so because of release of freezing of dipole behaviour up to transition temperature. Above transition temperature, dielectric value decreases with increasing temperature due to disappearance of domains as shown in figure 6.6 (a-e). The transition temperatures of all compositions are found below the room temperature which depicts their paraelectric phase at and above room temperature.

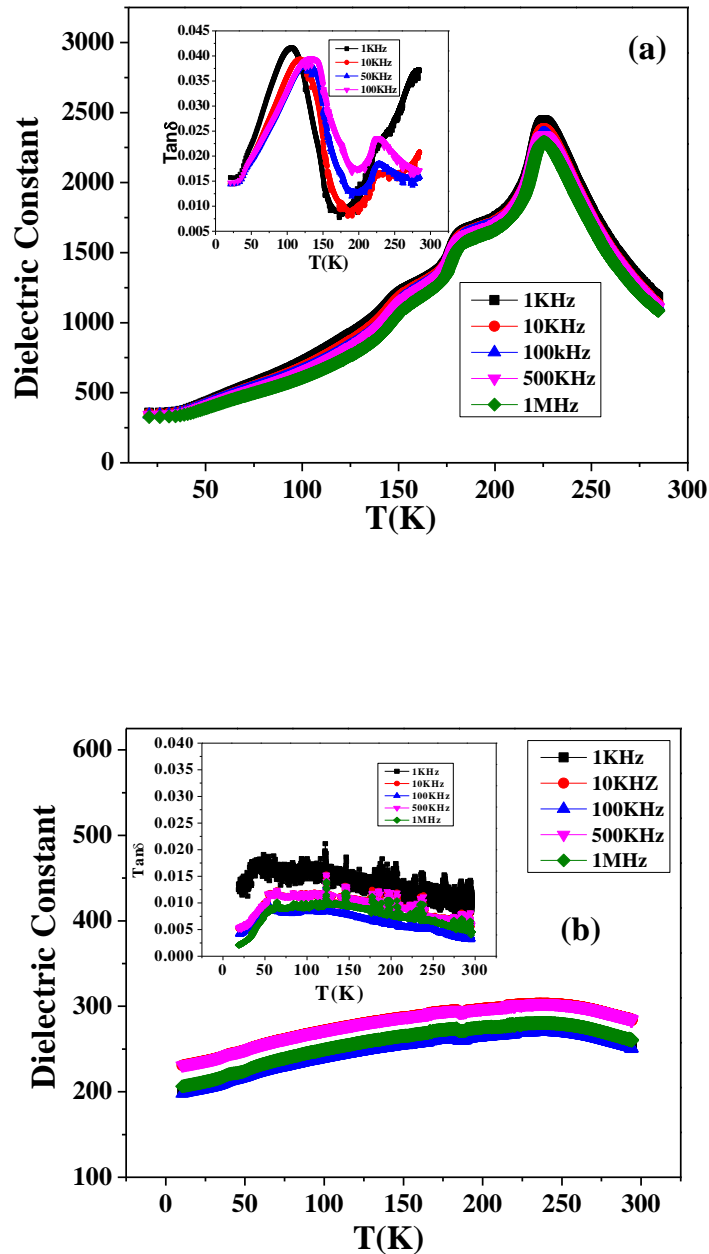
BaTiO<sub>3</sub> shows three polymorphic transitions at 393K, 288K and 197K [Jona and Shirane (1993)]. Due to doping of 0.5 mole fraction strontium at Ba site, the transition temperature shifts to 225K, 182K and 152K, respectively as shown in figure 6.5(a). The transition temperature shifts due to phase transformation within the BST sample. The ferroelectric to paraelectric phase transitions for BST-3B, BST-5B, BST-8B and BST-10B samples are found at 241K, 248K, 234K and 231K respectively.

Figure 6.7, presents the variation of dielectric constant with temperature for BST, BST-3B, BST-5B, BST-8B and BST-10B samples, It is observed that the dielectric constant value first increases with increasing BB glass (45Bi<sub>2</sub>O<sub>3</sub>-55B<sub>2</sub>O<sub>3</sub>) concentration up to (8wt%) and then decreases up to 10 wt% (BST-10B). When a small amount of glass (3wt%) is added to BST, the dielectric constant decreases by large amount due to introduction of other phase (glass with low dielectric) which causes decrease in effective dielectric constant by mixture rule. By increasing the glass concentration up to 5wt%, the transition temperature shifted towards higher temperature. Transition temperature shifts towards

lower temperature through further increase of glass concentration (> 5wt%). The shifting of transition temperature towards higher temperature may be due to the Bi content of glass trying to enter into the lattice of BST. The increasing concentration of glass above 5% leads to transient liquid phase and swelling of compact causing decrease in density, which leads to shifting of transition temperature towards causing lower temperature side. Insets of figures 6.5(a-e) and 6.6(a-e) show the variations of loss tangent with temperature.

The dielectric measurement at microwave frequency was performed using Keysight Technologies make Network Analyser [E5071C] and calibration kit X11664A. The Nicholson-Ross-Wier (NRW) technique was used for the measurement. Figure 6.8(a) shows the variation of dielectric constant as a function of frequency within the microwave frequency range 8.5 - 12 GHz at room temperature. The average dielectric constant value and dielectric loss of the prepared ceramic batches (BST, BST-3B, BST-5B, BST-8B and BST-10B) are reported in Table.6.3. It is observed that dielectric constant decreases almost linearly with increase in frequency. The decrease of dielectric constant at higher frequencies might be due to absence of interfacial and dipole polarizations as well as presence of heterogeneous distribution of charge carriers [Kamba et al. (2007)]. The dielectric constant values of all samples are very low at gigahertz frequencies, when compared with MHz or lower frequencies because of only dipole polarizations contributing significantly to dielectric constant at gigahertz frequencies. It is also observed from the graph that dielectric constant increases with increase in glass concentration up to BST-5B (5 wt%) and then it starts decreasing with further increase in glass concentration up to 10 wt% (BST-10B). The variations of loss tangent as a function of frequency for different glass concentrations are shown in figure 6.8(b). BST-5B shows

the highest dielectric constant of 43.2 and BST-3B shows lowest dielectric loss ( $\tan\delta \sim 0.169$ ) as compared with other glass added BST compositions.



**Figure 6.5** Variations of dielectric constant and loss tangent with temperature within the temperature range 20K - 293K at different frequencies for ceramic sample (a) BST, and (b) BST-3B.

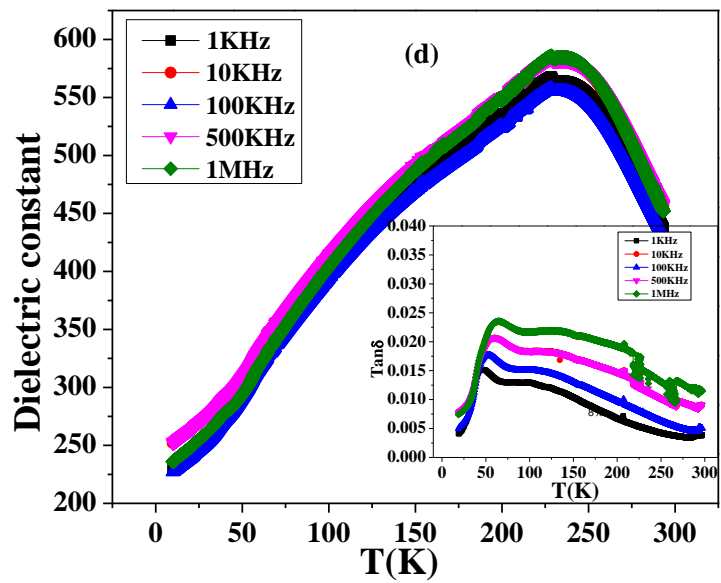
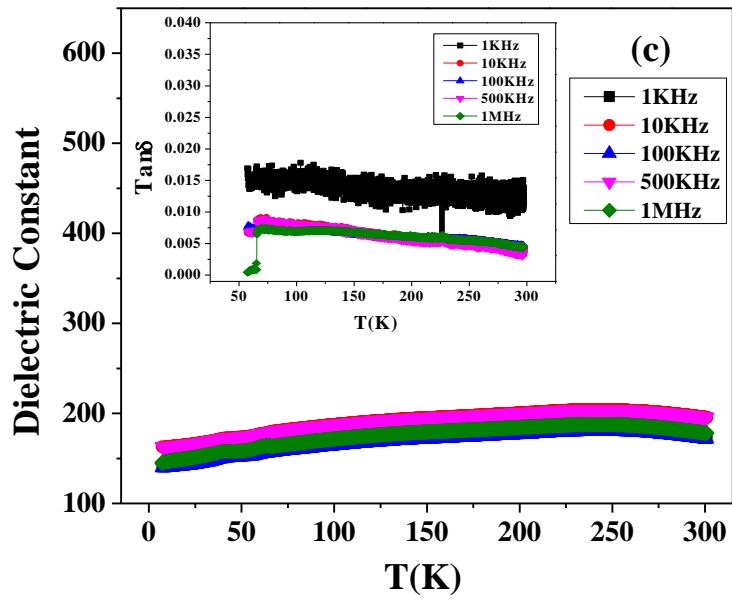


**Figure 6.5 (contd):** Variations of dielectric constant and loss tangent with temperature within the temperature range 20K - 293K at different frequencies for ceramic sample (c) BST-5B, and (d) BST-8B

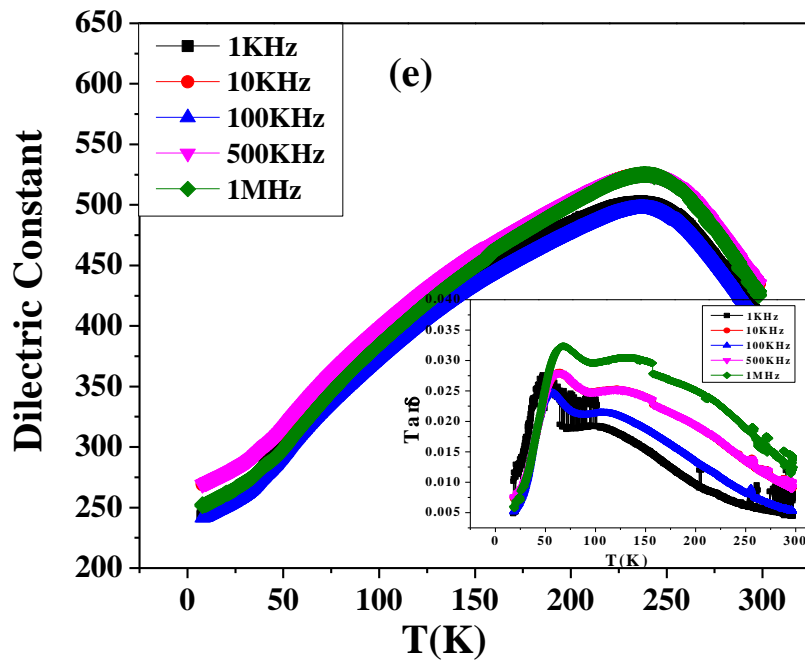


**Figure 6.5 (contd.):** Variations of dielectric constant and loss tangent with temperature within the temperature range 20K - 293K at different frequencies for ceramic sample (e) BST-10B.

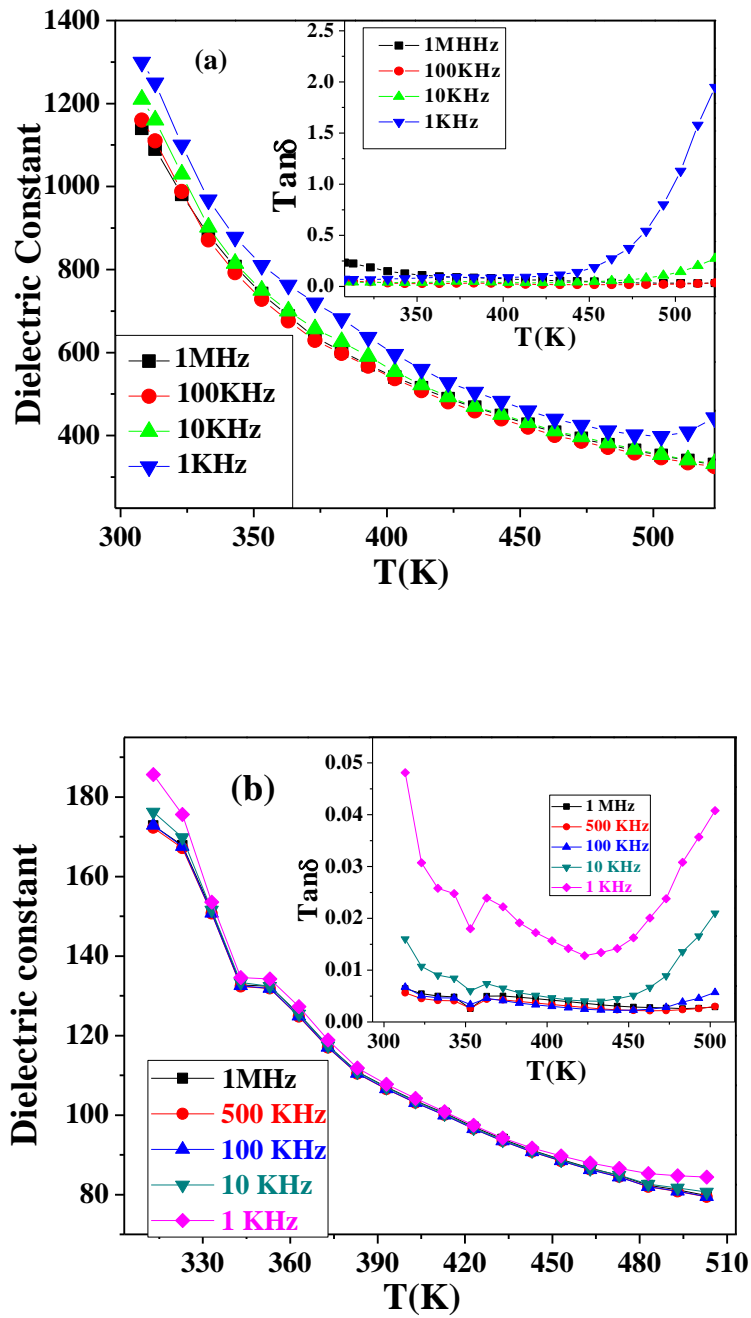


**Figure 6.6** Variations of dielectric constant and loss tangent with temperature within the temperature range 293K - 450K at different frequencies for ceramic sample (a) BST and (b) BST-3B.

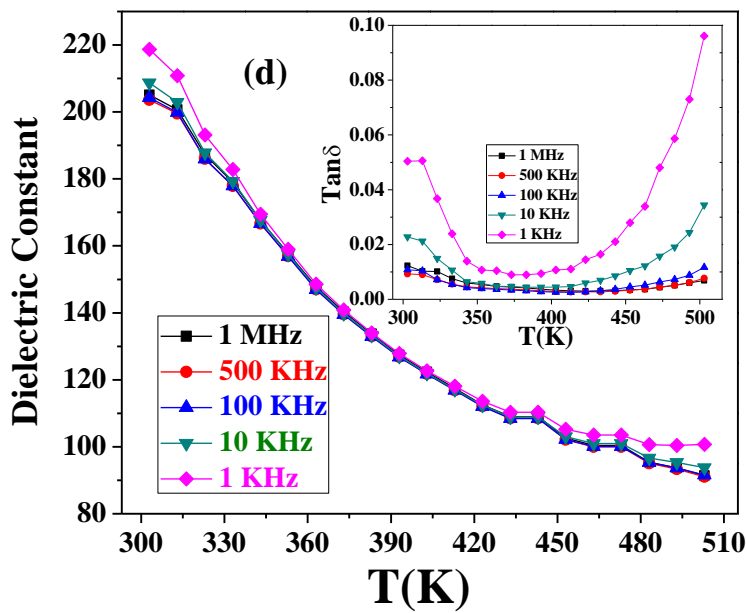
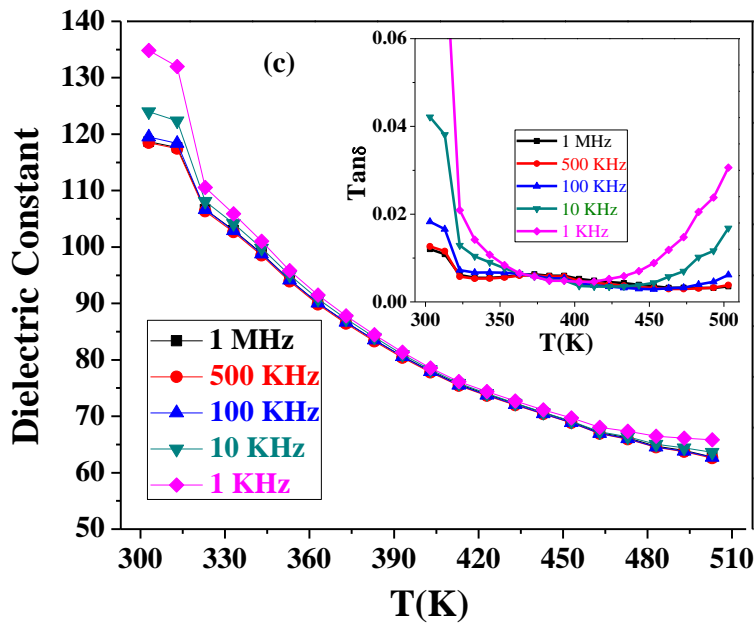


**Figure 6.6 (contd.)** Variations of dielectric constant and loss tangent with temperature within the temperature range 293K - 450K at different frequencies for ceramic sample (c) BST-5B, and (d) BST-8B.

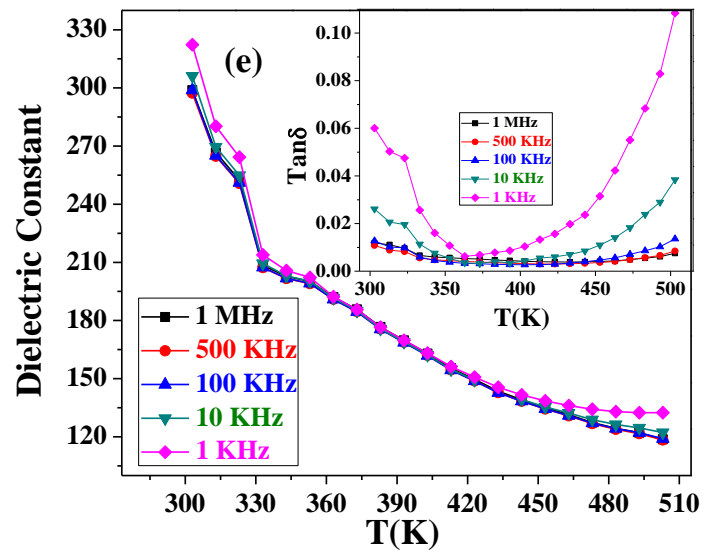


**Figure 6.6 (contd.)** Variations of dielectric constant and loss tangent with temperature within the temperature range 293K - 450K at different frequencies for ceramic sample (e) BST-10B.

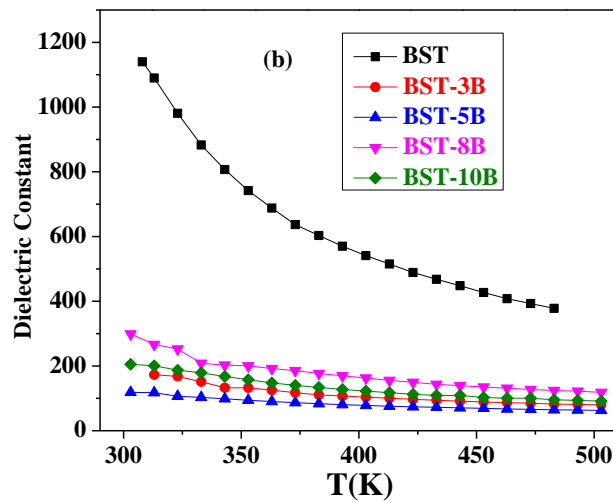
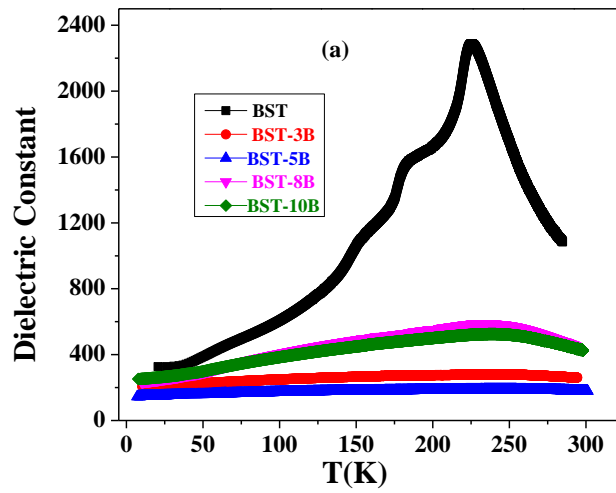


**Figure 6.7** Variations of dielectric constant for different ceramic samples at 1 MHz in the temperature range (a) 20 - 293K and (b) 293K - 450K.

**Table 6.3** Dielectric properties of BST ceramic and BB glass added BST compositions within the frequency range (8.5 – 12 GHz)

S.No.	Material	Average dielectric constant	Average loss tangent
1.	BST	84.0	0.013
2.	BST-3B	17.0	0.169
3.	BST-5B	43.2	0.496
4.	BST-8B	37.1	0.328
5.	BST-10B	22.5	0.472

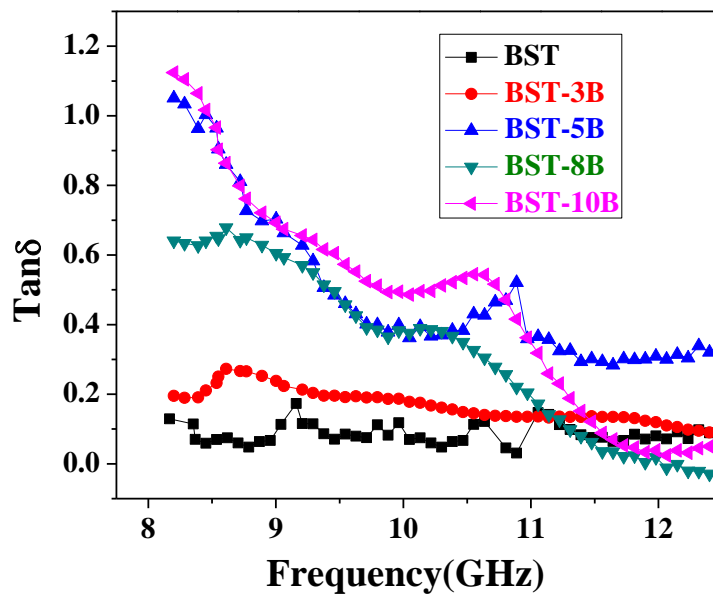
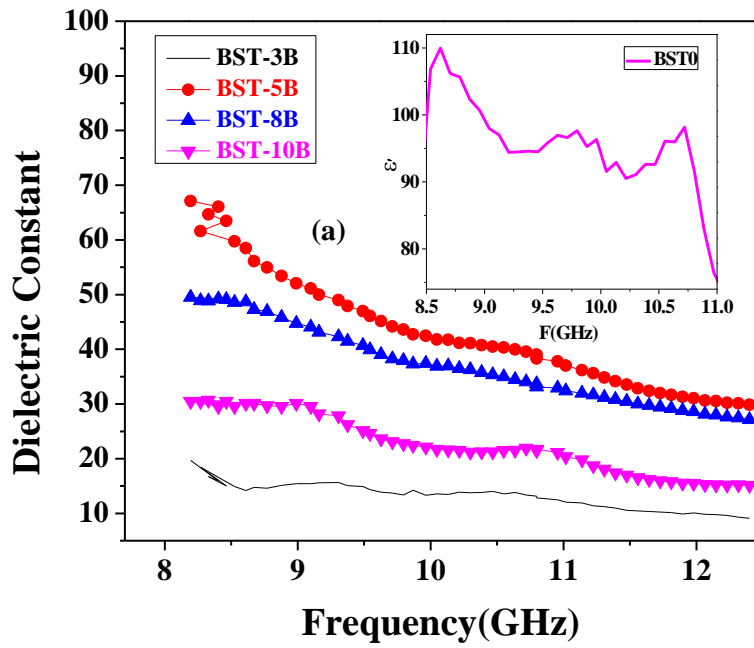


**Figure 6.8** Variations of (a) Dielectric constant, and (b) Loss tangent of different ceramic samples with frequency in GHz range.

### 6.3 Summary

In this chapter, effects of increasing amount (3, 5, 8 and 10 wt %) of BB glass additive on  $\text{Ba}_{0.5}\text{Sr}_{0.5}\text{TiO}_3$  (BST) ceramic have been investigated. Increasing weight percentage of BB glass additive significantly reduces the sintering temperature of BST. Composition BST-5B shows the highest density at sintering temperature of 1223 K as compared with all other compositions. XRD analysis has revealed that addition of BB glass has no effect on the crystal structure of BST. Analysis of dielectric property has revealed that transition temperature increases with increase in glass concentration up to 5 wt% and then it starts decreasing through further increase of glass concentration (>5 wt%). Dielectric constant and loss tangent of all glass added ceramics have been observed at lower frequencies (for different temperature range) and also in microwave frequency range 8.5-12 GHz (at room temperature). Highest dielectric constant value in microwave frequency range has been observed for BST-5B sample. Minimum dielectric loss value in microwave frequency range has been observed for BST-3B sample. Dielectric constant and loss tangent of glass added BST samples lie in the range 17 – 43.2 and 0.169 -0.496 respectively. Therefore, low loss ceramic material with dielectric constant in the range of 17 - 43.2 can be potentially useful for the design of microwave dielectric resonator antennas. Among all composition, **BST-3B** ceramic has been used for design and development of CDRA (detailed description present in chapter 7).